

CAAP Quarterly Report

Date of Report: 12/29/2020

Prepared for: *U.S. DOT Pipeline and Hazardous Materials Safety Administration*

Contract Number: 693JK31950008CAAP

Project Title: Distributed Fiber Optic Sensor Network for Real-time Monitoring of Pipeline Interactive Anomalies

Prepared by: Dr. Yi Bao and Dr. Ying Huang

Contact Information: Email: yi.bao@stevens.edu, Phone: (201) 216-5223

For quarterly period ending: 12/31/2020

Business and Activity Section

(a) Contract Activity

Discussion about contract modifications or proposed modifications

None.

Discussion about materials purchased

None.

(b) Status Update of Past Quarter Activities

High level summary of the work performed for the reporting period.

In the fifth quarter, the university research team partially completed Task I, Task II, and Task IV of the above-mentioned project, including experimental testing on FBGs subjected to loading and loading & corrosion and distributed fiber optic sensors subjected to corrosion, in addition to advising two graduate students and five undergraduate students.

(c) Cost share activity

None.

(d) Task I: Developing and Characterizing Distributed Fiber Optic Sensors

In Task I, we aim to develop and characterize distributed fiber optic sensors under (i) deformation, (ii) corrosion, and (iii) excavation, as well as (iv) conducting a sensitivity study. In the fifth quarter, corrosion tests were conducted to test the performance of distributed fiber optic sensors for detecting and locating corrosion in steel pipes; and two graduate students and two undergraduate students were trained to conduct experimental testing of fiber optic sensors.

Detailed discussion and descriptions for the following:

1. Background

In the last quarterly report (the fourth report for July 1, 2020 to September 30, 2020), distributed fiber optic sensors were shown to be promising for measuring corrosion condition. Although in previous research, it was found that fiber optic sensor showed feasibility of the detection corrosion. However, interaction between loading and corrosion using fiber optic sensors was not fully investigated through experimentation. In this study, the research team conducted corrosion tests of steel pipes instrumented with distributed fiber optic sensors, based on the OFDR technology with an improved spatial resolution (down to 0.65 mm) [1].

2. Objectives

In the fifth quarterly research, the research team aims to detect and locate corrosion of steel pipes using distributed fiber optic sensors.

3. Experimental program

3.1. Optical fibers

This study investigates three types of telecommunication-grade single-mode optical fibers as distributed fiber optic sensors, including a bare fiber and two coated fibers, as depicted in Fig. 1. In this study, the optical fiber serves as a distributed sensor and the transmission line. The bare fiber is composed of a glass core (diameter: 9 μm), a glass cladding (diameter: 125 μm), an inner coating (diameter: 190 μm), an outer coating (diameter: 242 μm). Light waves propagate along the optical fiber through total internal reflection at the core-cladding interface. The sensing part is the glass core and cladding. The inner coating is a soft acrylic layer which protects the glass fiber from mechanical impact, and the outer coating is a stiff acrylic layer which protects the glass from abrasion and environmental exposure. To further enhance the mechanical strength and facilitates operation of the fiber in practice, the coated fibers are packaged with tight buffers in addition to the bare fiber. In this study, the two types of coated fibers with tight buffers measured 650 μm and 900 μm in diameter are investigated, respectively.

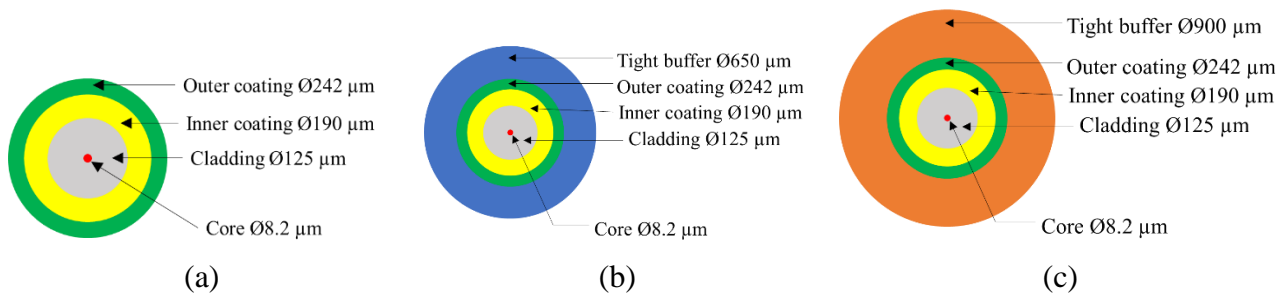


Fig. 1. Cross section of the bare fiber and fiber coated with tight buffer: (a) 242- μm -diameter bare fiber; (b) 650- μm -diameter coated fiber; and (c) 900- μm -diameter coated fiber.

3.2. Materials and specimen preparation

Fig. 2 shows the selected pipe segments. The selected materials of the pipe segments are normal steel and stainless steel, which can be used for the transmission of air, natural gas, oil, steam, and water by following ASTM A733 and ASTM A269. The diameter of pipe segments is 25.4 mm (1 inch) and the thickness is 3 mm (0.12 inch). Each pipe segment is cut into 300 mm in length.

Normal steel

Stainless steel



Fig. 2. Selected pipe segments: (a) normal steel pipe; and (b) stainless steel pipe.

Before installation of optical fibers, the corrosion and rust on the external surface of pipe segments are removed and cleaned with alcohol wipes. The next step is to tape down the fiber sensor in the desired layout across the pipe segments. In this step, tape dots are used to hold the fiber in place. The final step is to apply adhesive to the sensor and cure it onto the test surface. The bond line quality will ultimately determine the efficiency of strain transfer from the test article to the fiber sensor. As long as enough epoxy is used to cover the fiber sensor, the efficiency of strain transfer is not affected by excessive adhesive. However, the bond thickness (amount of epoxy between the fiber and the surface) should be minimized to ensure that the fiber is truly resting on the surface of the pipe segments.

3.3. Investigated cases

This research investigates the effects of the coating thickness, spatial resolution, installation patterns, and spacing between the helix fiber. A total of 16 cases are investigated, including 3 coating thicknesses (242 μm , 650 μm , and 900 μm), 6 spatial resolution (0.65 mm, 1.3 mm, 2.6 mm, 5.2 mm, 10.4 mm, and 20.8 mm), and 3 installation patterns (spiral pattern, line pattern, and spiral+line pattern), and 6 spacings between the helix fiber (10 mm, 20 mm, 40 mm, 60 mm, and 80 mm).

The control case uses a bare fiber (coating thicknesses 900 μm) and the spatial resolution of 0.65 mm. Four steel pipe specimens were prepared and instrumented with distributed fiber optic sensors, namely P0, P1, P2, and P3. Among them, the specimen P0 is stainless steel pipe, which is used as the control; and the specimens P1, P2 and P3 are normal steel pipe, which are used as study group. The specimen P0 was instrumented with coated fiber with 900- μm diameter tight buffer in spiral pattern, and the spacing between the helix fiber is 20 mm. The specimen P1 was instrumented with three types of distributed sensors (Fig. 1) in spiral pattern with 20 mm spacing. The specimen P1 is used to investigate the effects of coating thickness, and both the specimens P0 and P1 can be used for the investigation of spatial resolution on precision of corrosion condition mapping, which is shown in Fig. 3(a). The specimen P2 was instrumented with coated fibers with 900- μm diameter tight buffer in spiral+line pattern in order to investigate the effects of installation patterns, which is shown in Fig. 3(b). the spacing between the helix fiber for the specimen P2 is also 20 mm, and the line pattern divide the circumference of the specimen P2 into three equal parts. The specimen P3 was instrumented with five 900- μm -diameter-tight-buffer coated fibers in different spiral patterns. Five spacings between the helix fiber are investigated, which is shown in Fig. 3(c).

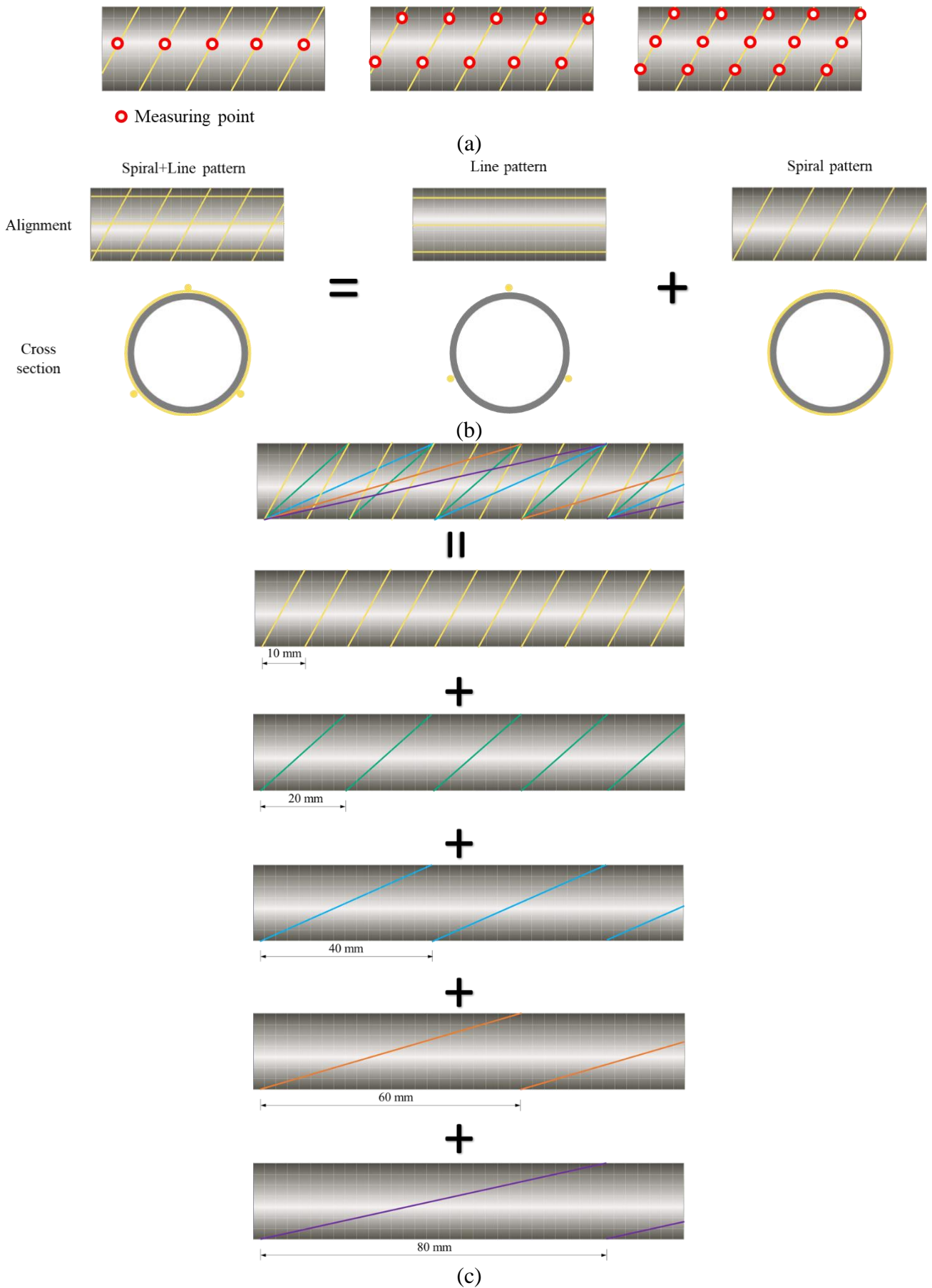


Fig. 3. Instrumentation of: (a) the specimen P1 for investigating spatial resolution; (b) the specimen P2 for investigating installation patterns; and (c) the specimen P3 for investigating installation patterns.

3.3.4. Investigated cases

After the adhesive (superglue) get solidified for two hours, pipe segment specimens were immediately immersed in 3.5 wt. % sodium chloride solution. Then, the corrosion test was conducted, as shown in Fig. 4. For each specimen, optical fibers installed on the pipe segment were connected to a OFDR data acquisition system for measurement, as shown in Fig. 4(a). The spatial resolution was set at 0.65 mm, meaning two points with a distance no less than 0.65 mm could be differentiated. Each measurement took about 20 s to 40 s, and each measurement was repeated for three times, and the measurement results were averaged.

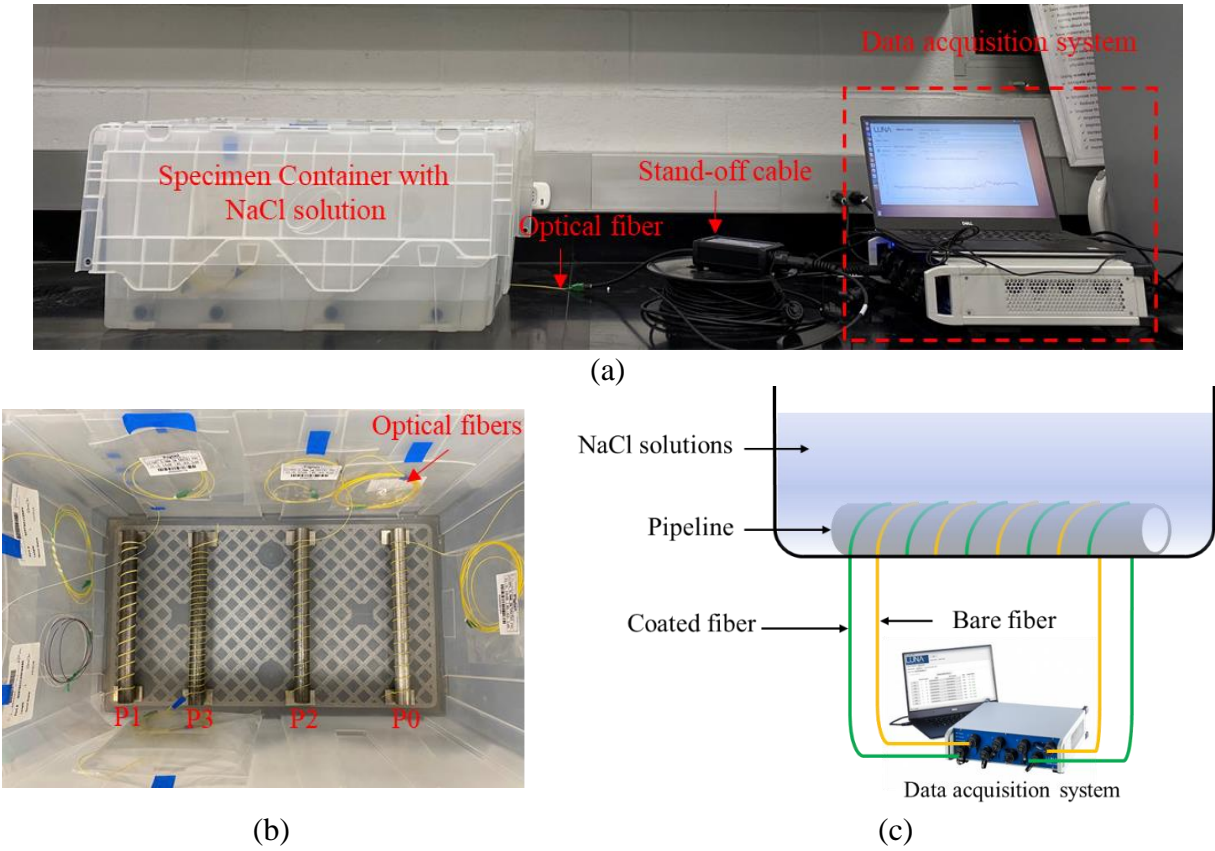


Fig. 4. Experimental test of corrosion: (a) test set-up; (b) specimens in the chamber; and (c) illustration of steel pipe instrumented with a distributed fiber optic sensor.

3.3.5. Experimental results

During the corrosion tests, the surface condition of the tested pipe segment specimens was visually inspected at different times, as shown in Fig. 5. As the time continues, rust was observed on the surface of P1, P2, and P3; however, little rust was found on the on the surface of P0, which can be attributed to the use of the stainless steel of P0.

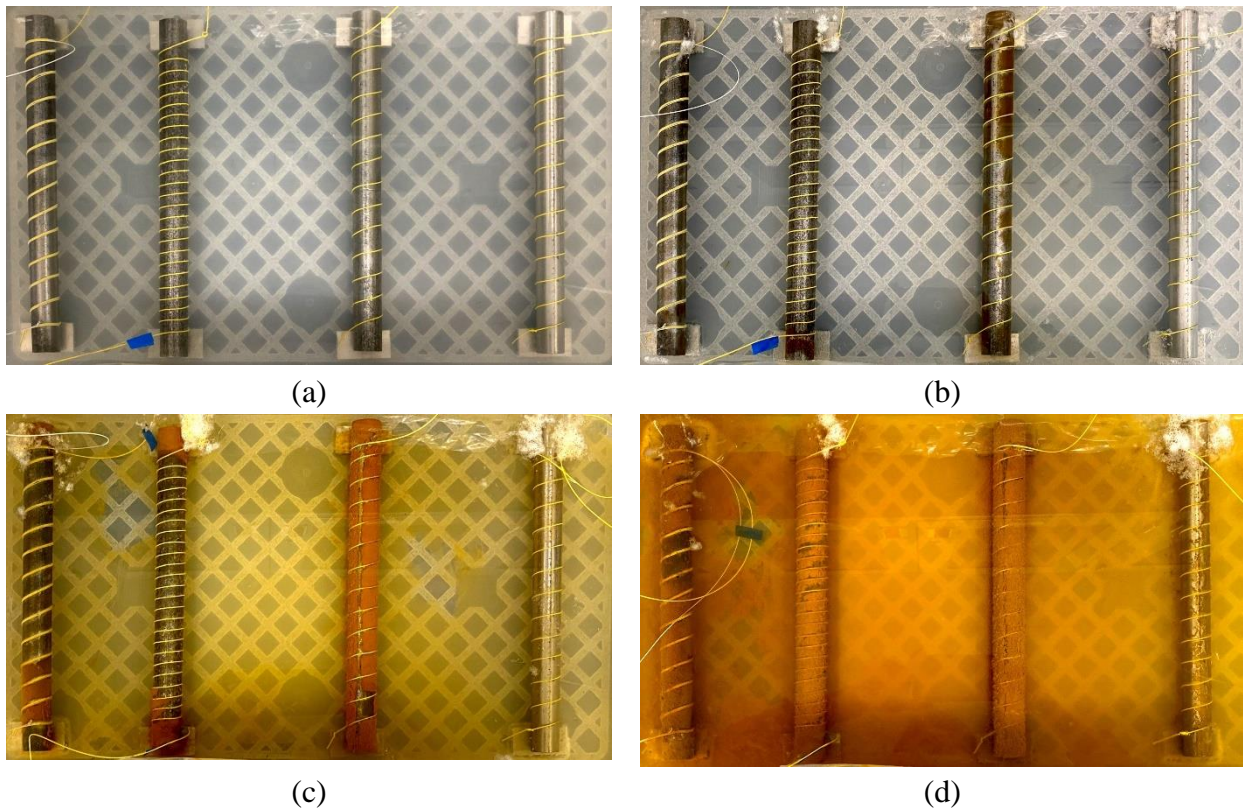
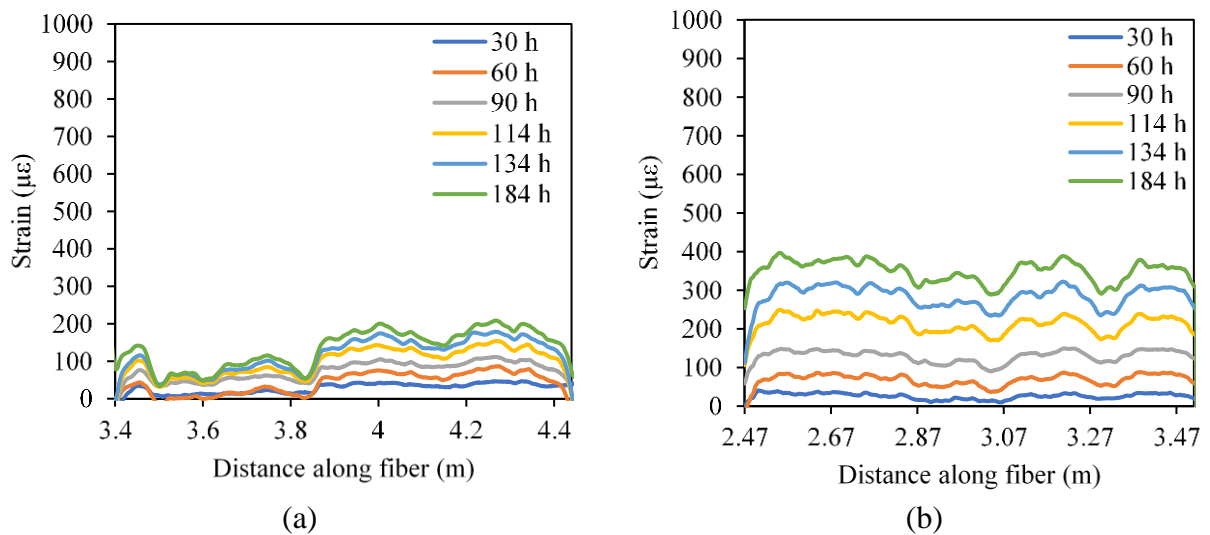
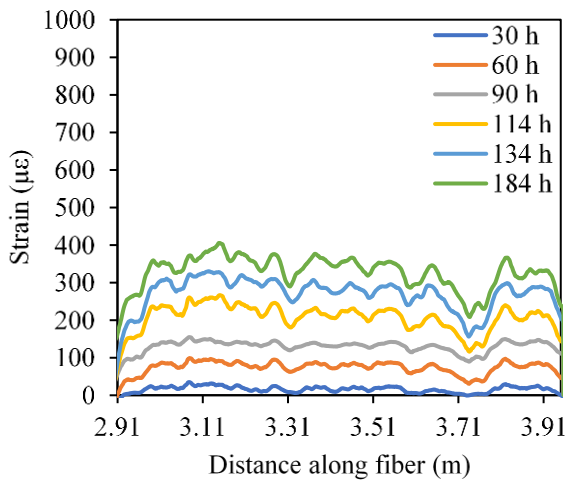


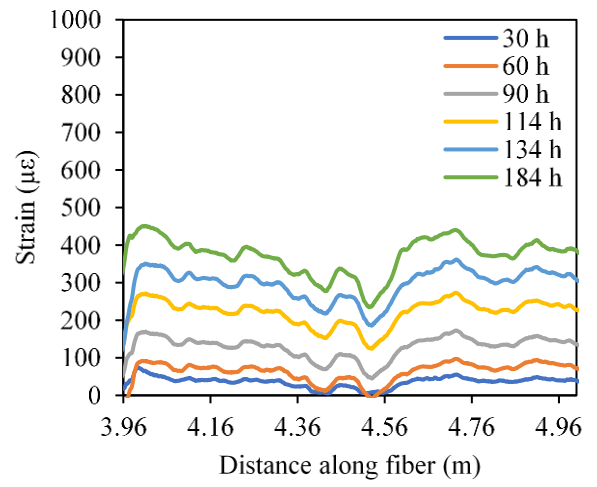
Fig. 5. Visual observation of the pipe segments in different times: (a) 30 h (hour); (b) 60 h; (c) 114 h; and (d) 184 h.

Fig. 6 shows the corrosion-induced expansion strain measured from the distributed sensors installed on the pipe segment specimens. The Y-axis represents the strain measured from the distributed sensor; tensile strain is positive. The X-axis represents the position along the length of the optical fiber. In each figure, the length range of the optical fiber is selected to show the strains in the fiber length that are wrapped on the pipe segment specimens.

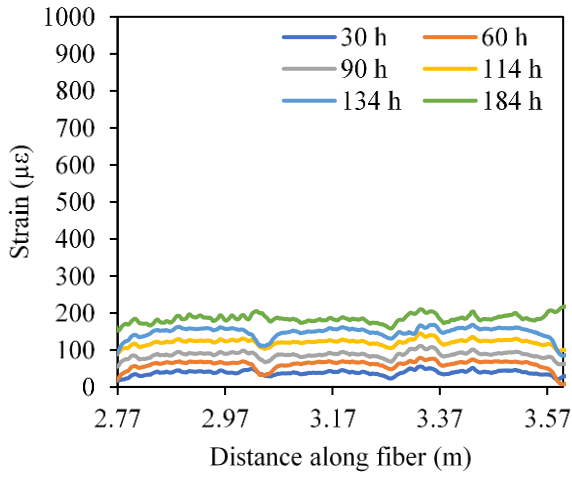




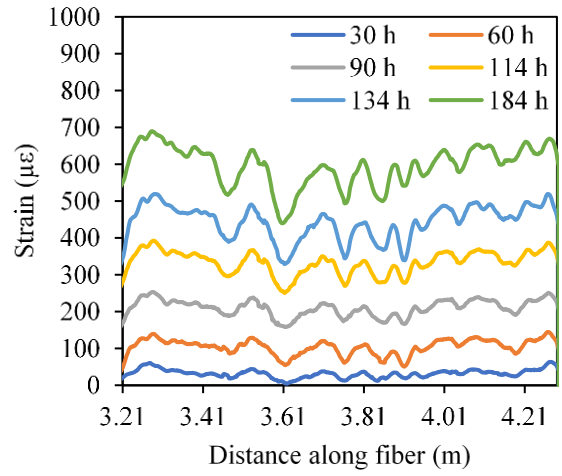
(c)



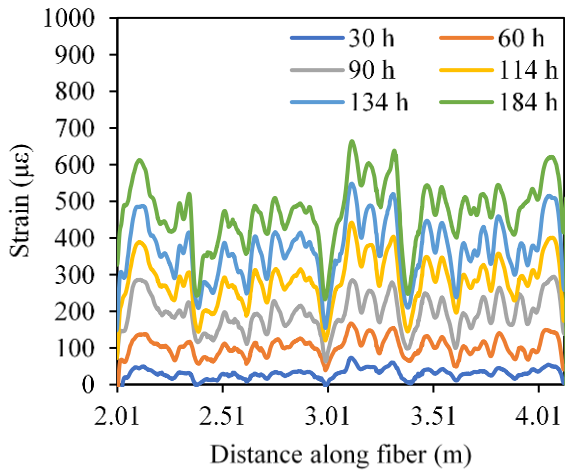
(d)



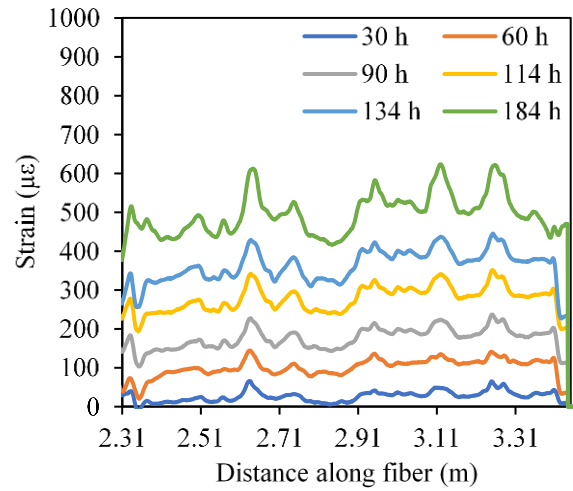
(e)



(f)



(g)



(h)

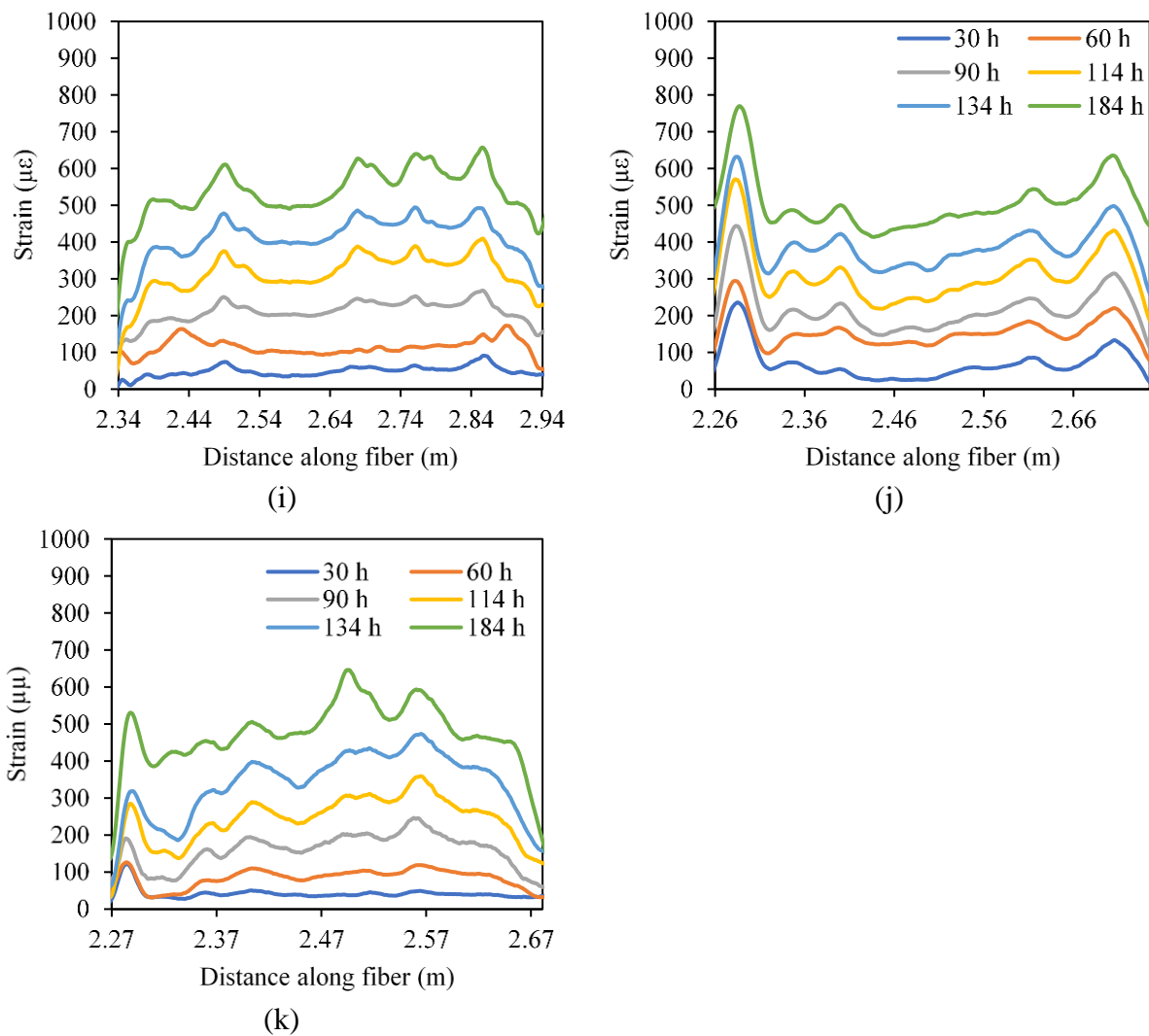


Fig. 6. Detailed strain distributions along the distributed sensors in the pipe segment specimens: (a) P0; (b) P1-242 μm ; (c) P1-650 μm ; (d) P1-900 μm ; (e) P2-line pattern; (f) P2-spiral pattern; (g) P3-10 mm; (h) P3-20 mm; (i) P3-40 mm; (j) P3-60 mm; and (k) P3-80 mm.

(e) Task II: Developing and Characterizing Point Fiber Optic Sensors

In Task II, we aim to develop and characterize point fiber optic sensors. In the fifth quarter, three activities were performed for Task II, including (1) using FBGs to monitor the wavelength shifts of steel plates coated with epoxy under loading; (2) using FBGs to monitor the wavelength shifts of steel plates coated with epoxy under corrosion; and (3) trainings of two graduate students and five undergraduate students for experimental testing of fiber optic sensors.

Detailed discussion and descriptions for the following:

1. Background

In the last quarterly report (the fourth report for July 1, 2020 to September 30, 2020), point fiber optic sensors were shown to be promising for measuring corrosion condition. Although in previous research, it was found that fiber optic sensor showed feasibility of the detection corrosion. However, interaction between loading and corrosion using fiber optic sensors was not fully investigated through experimentation. In this study, the research team derived the interaction between loading and corrosion by monitoring the wavelength shifts of steel plates coated with epoxy under loading and corrosion.

2. Objectives

In the fifth quarterly research, there were two main objectives: (1) using FBGs to monitor the wavelength shifts of steel plates coated with epoxy under loading; and (2) using FBGs to monitor the wavelength shifts of steel plates coated with epoxy under loading and corrosion, in order to derive the interaction between loading and corrosion.

3. Experimental program

3.1. Test of Packaged FBGs

Based on the previous test design and tube length design, following are the loading test results of FBGs packaged with PTFE tubes (SWTT-30). The dimension of SWTT-30 was 0.012"×0.021" (inner diameter × outer diameter).

3.1.1 Sample of FBG with PTFE tube (SWTT-30)

The preparation of experimental samples was similar to that of the samples with bare FBG sensors, but the FBG sensors were packaged with the PTFE tubes (SWTT-30). First, an FBG sensor was inserted into a 4" PTFE tube. Then, the sensing length of the sensor was stretched to be straight and then attached to a ruler with a tape. The center point of the sensing length was marked using a marker, in order to ensure that the center point of the sensing length coincided with the center point of the tube. After fixing the position of the tube, a glue was used to attach the two ends of the tube with the FBG sensor. The completed samples are shown in Fig. 8. They are designated as S30-1, S30-2, S30-3, and ST30-0.

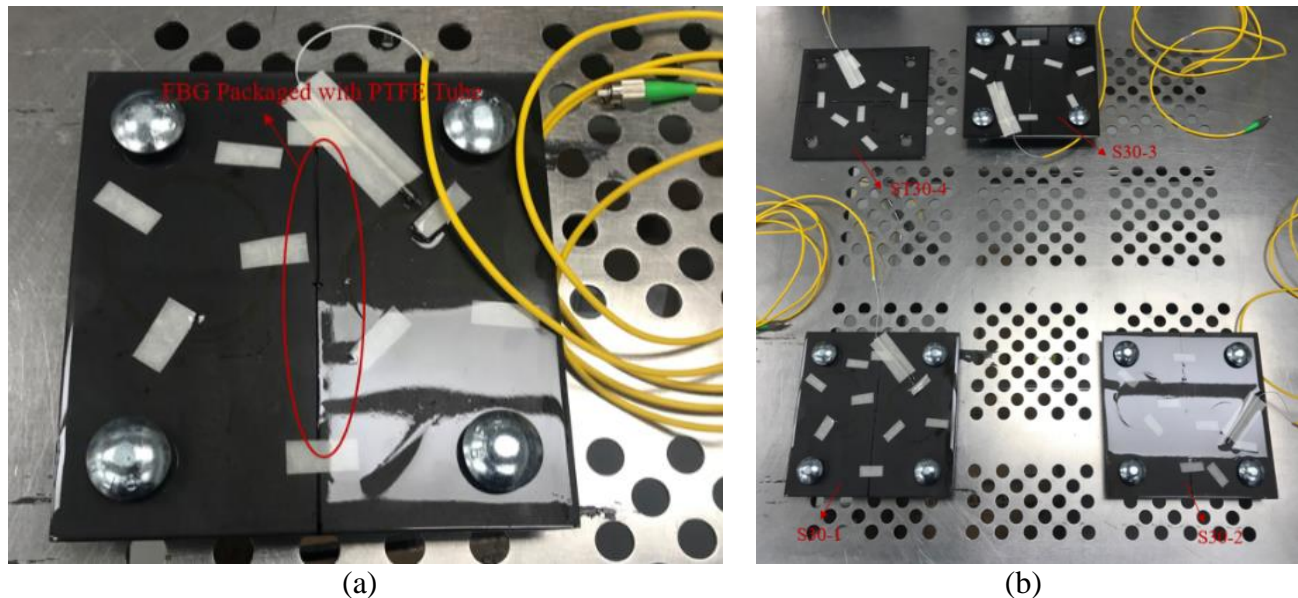


Fig. 8. Samples of FBGs packaged with PTFE tubes.

3.1.2. Loading test of FBG with PTFE tube (SWTT-30)

Using the stainless-steel frame with a 6"×6"×0.125" stainless-steel plate and a diameter of 3/4" stainless-steel bar to achieve the loading test. After fixing the frame with tape on the top surface of steel plates where FBG sensors have been embedded, put stainless-steel plates on the stainless-steel frame step by step to achieve the stepwise application of five-level load, as shown in Fig. 9.

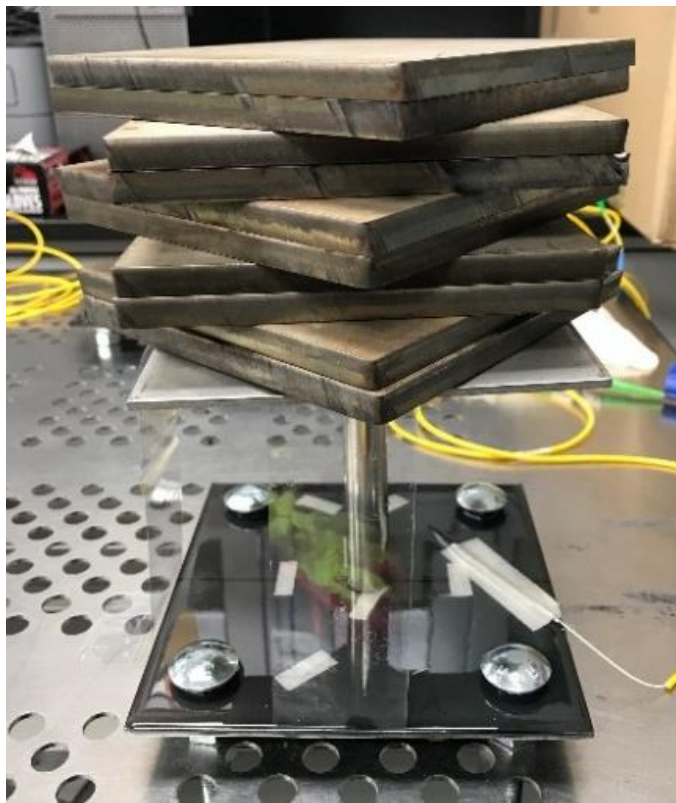
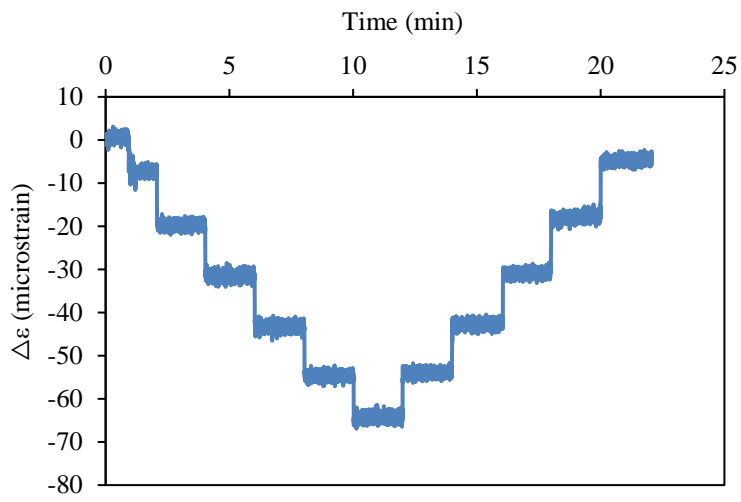


Fig. 9. Test set-up of the crack testing.

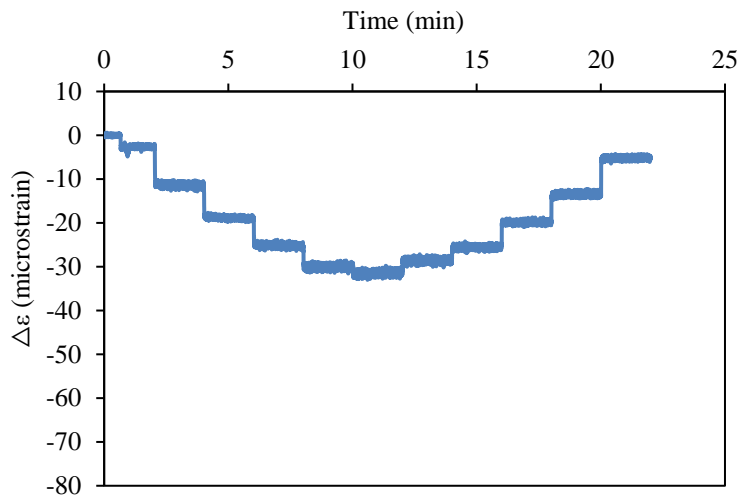
3.1.3. Loading test results of FBG with PTFE tube (SWTT-30)

Fig. 10 shows the results of strains measured from the FBG sensors in the three specimens (i.e., S30-1, S30-2, and S30-3). Each level of load was sustained for about 2 minutes. At each load level, the strains in the steel plate were measured using the FBG sensor attached on the steel plate. According to the test design, the increment of the strain for adjacent load levels was $20 \mu\epsilon$ (micro-strains). However, in the actual test, the measured strains from the FBG sensors in the three specimens were much smaller than the theoretical results. Specifically, the total strains measured from the sensors S30-1, S30-2, and S30-3 were $65 \mu\epsilon$, $32 \mu\epsilon$, and $20 \mu\epsilon$, respectively, while the theoretical strain was $120 \mu\epsilon$. The lower strain results were attributed to multiple reasons. On one hand, the package of the tube led to strain transfer effect, which could lead to smaller strains sensed by the FBG sensor. On the other hand, based on the observation of the test processes and the specimens, it was found that the FBG sensors were not straight after they were packaged by the tubes and attached on steel plates, which explained why the measured strains were different in the three specimens.

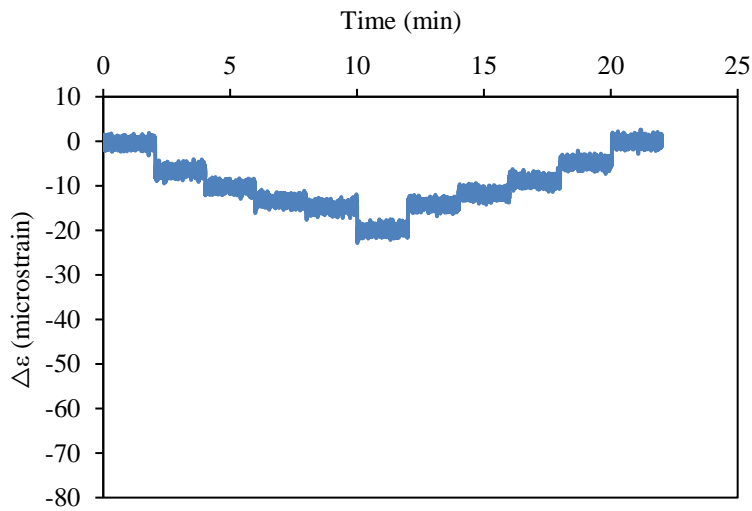
Based on the above experience, it was learned that a certain prestress should be applied to ensure that the FBG sensor would be straight throughout the sensor preparation process. The prestress should be small and does not affect the measurement, but it should be large enough to keep the sensor straight, in order to achieve a reasonable measurement performance.



(a)



(b)



(c)

Fig. 10. Loading test results of steel plates with SWTT-30 packaged FBGs (Microstrain vs. Time): (a) S30-1; (b) S30-2; and (c) S30-3. The results are presented after performing temperature compensation.

3.2. Loading and Corrosion Test of Bare FBG

3.2.1. Loading and Corrosion test design of bare FBG

Because this research is based on the test of steel corrosion under soft coating, and the soft coating (epoxy) is difficult to produce damage without external force. In order to accelerate the occurrence of steel corrosion, it is necessary to deliberately make a crack in the coating at the beginning of tests. The test when there was no crack in the coating was used as the control. Then, a crack was made parallel to the FBG. It is a long process to make the samples with epoxy to corrode in the 3.5wt% sodium chloride (NaCl) solution, so the test will be continued for 120 days. Meanwhile, to monitor the interaction between loading and corrosion at different periods and degrees of corrosion, a five-level loading is applied to the specimens every six days. The experimental schedule is listed in Table 1.

Table 1. Experimental Schedule of Loading & Corrosion Test

Time (Days)	Test Operation
Day 0	Test Start
Day 1	Making Cracks
Day 4	Loading Test
Day 10	Loading Test
Day 16	Loading Test
...	...
Day 118	Loading Test
Day 120	Test End

3.2.2. Loading & Corrosion test setup of bare FBG

To simulate the real corrosive environment and achieve real-time monitoring of corrosion, PVC pipes with a diameter of 4 inches were attached to the top surface of the steel plates with FBG sensors and filled with 3.5 wt. % sodium chloride (NaCl) solution. The test setup of loading and corrosion is shown in Fig. 11.

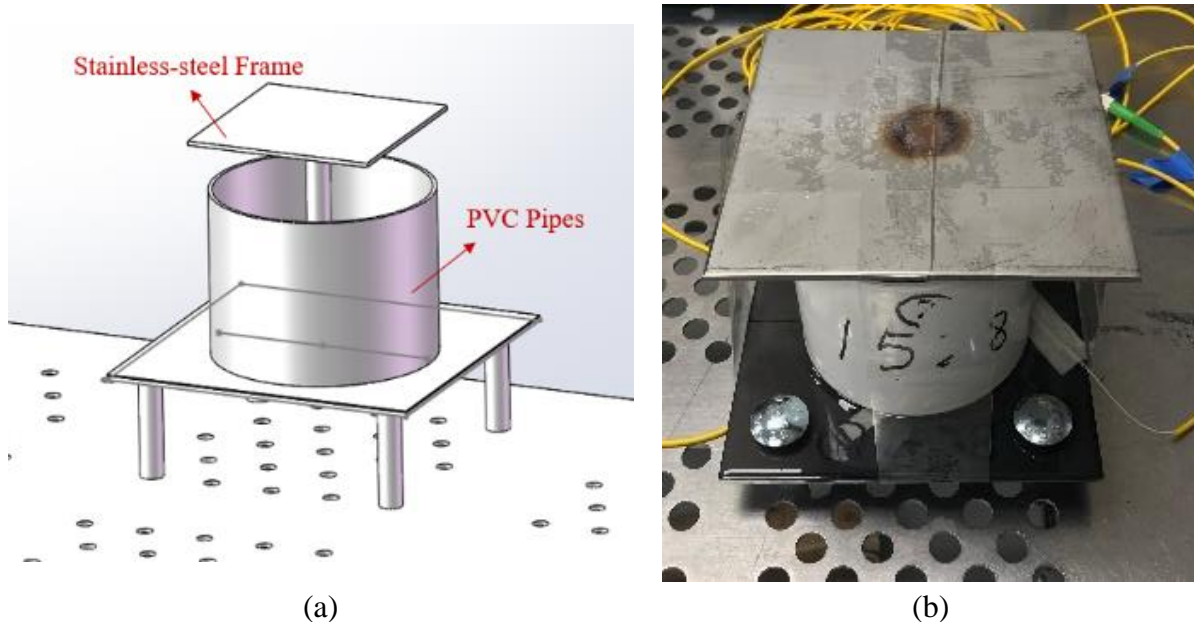


Fig. 11. Depiction of the test set-up for loading and corrosion experiment using bare FBG sensors: (a) schematic illustration, and (b) photograph.

The five-level loading was applied and unloaded step by step by placing the stainless-steel plates on the frame, as shown in Fig. 12.

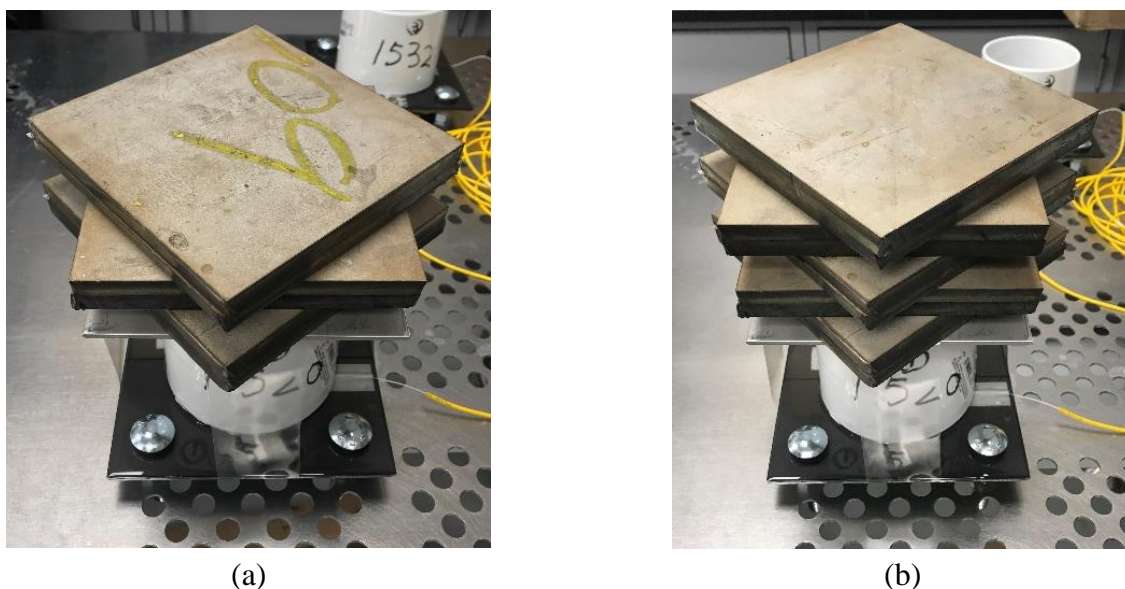


Fig. 12. Five-level loading: (a) the third level of loading, and (b) the fifth level of loading.

3.2.3. Loading & Corrosion test results of bare FBG

Fig. 13 shows the FBG interrogator. In the experiment, the specimens with bare FBG sensors B0, B1, B2, and B3 were connected to the different channels of the interrogator. Their center wavelengths were 1524 nm, 1520 nm, 1528 nm, and 1532 nm, respectively. The test is still on-going, so only a part of the test data are reported in the following.

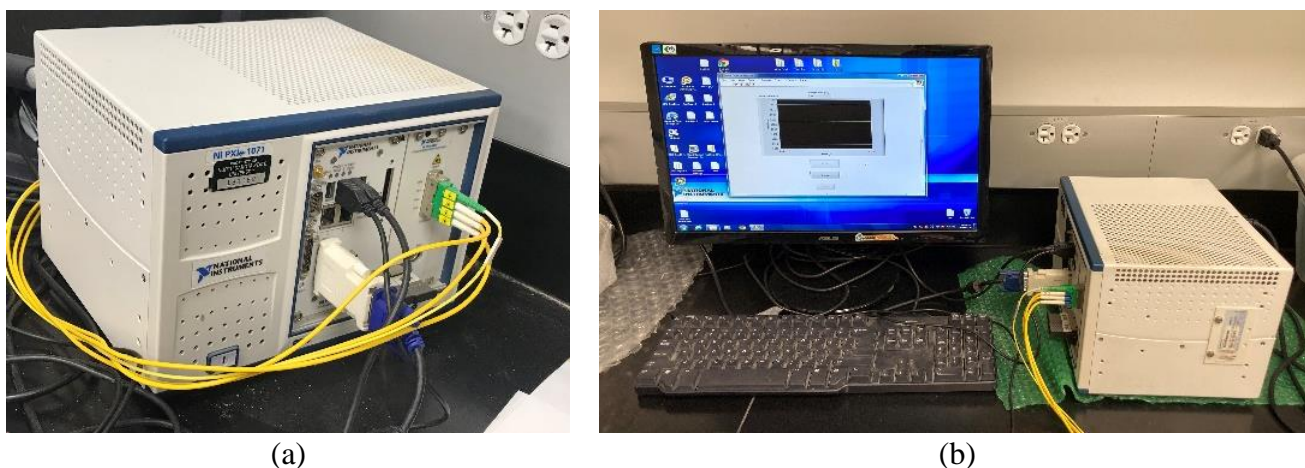


Fig. 13. Pictures of the interrogator: (a) the connection of the interrogator, and (b) the test set-up.

Fig. 14 shows the corrosion degree of three different samples at the beginning (day 0), making cracks (day 1), and the testing at 10 days, 30 day and 60 days. At 10 days, none of the samples showed any visible rust. At 30 days, all the three specimens showed minor corrosion. The specimens B1 and B2 produced brown-red corrosion products. The specimen B3 showed a small white area around the crack, indicating that the solution had entered the gap between the epoxy and the steel plate, but no corrosive product was observed. The reason for the differences in the corrosion degrees is that the cracks were man-made, so the sizes of cracks were different. At the same day, the corrosion severity was random in different specimens. At 60 days, the corrosion areas expanded, and the corrosion phenomenon became more obvious.

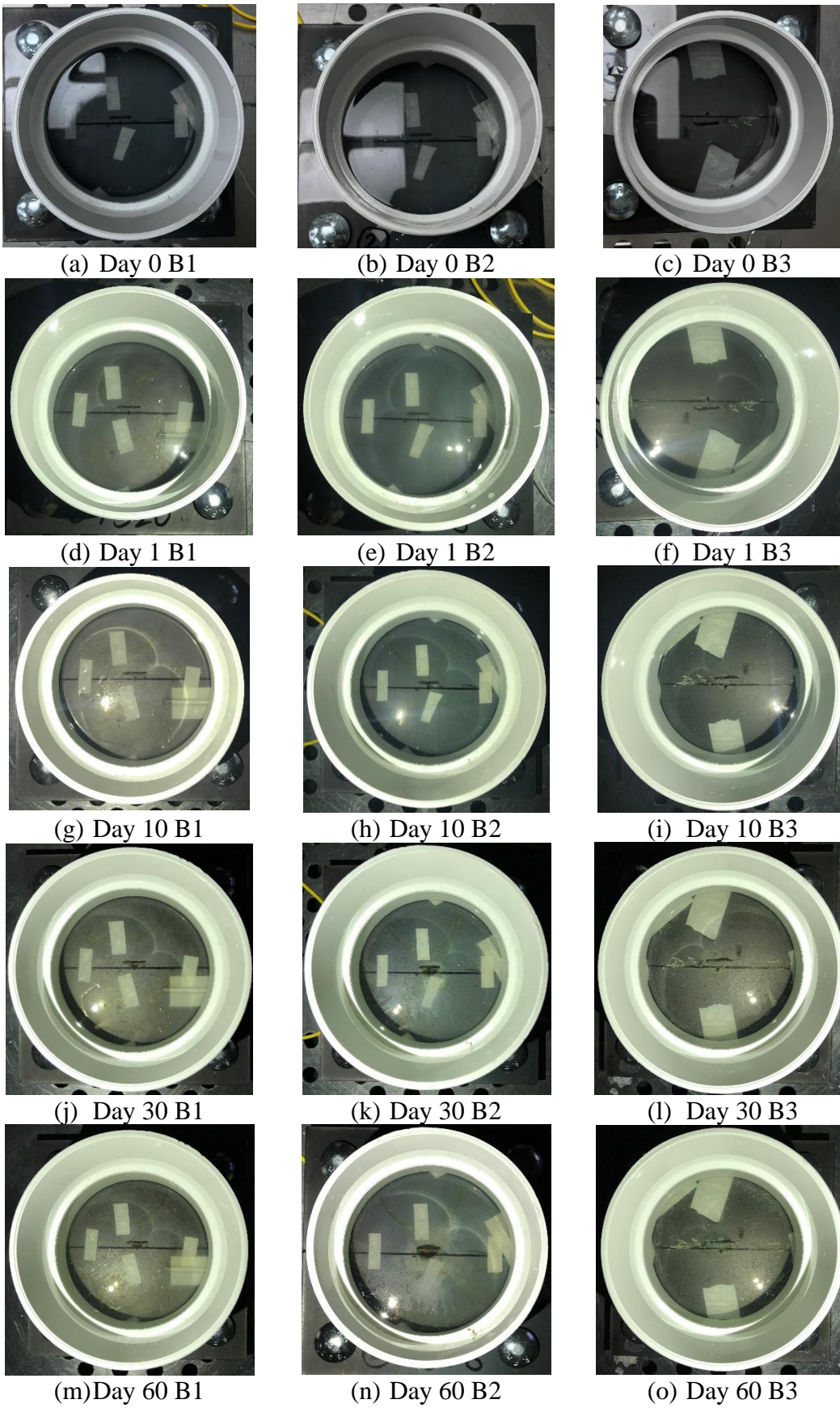


Fig. 14. Pictures of the tested specimens at different days (up to 60 days).

According to the monitoring of wavelength shifts, the wavelengths gradually decreased with time, indicating the occurrence of corrosion. The corrosive products were generated on the surfaces of steel plates, between the steel plates and epoxy, which exerted pressure to the FBG sensor. Therefore, the wavelengths showed gradual decrease. When the loading tests were conducted, the wavelength showed prominent peaks. The number of peaks indicated how many loading tests had been performed. There might be a larger peak or a smaller peak, due to the distribution of corrosive products when they were squeezed, so the FBGs might be compressed or elongated. In each loading and unloading process, the stepwise wavelength shifts could be seen, which are consistent with the results of loading tests. The wavelength shifts of three samples before temperature compensation and detailed diagrams of loading tests are shown in Fig. 15.

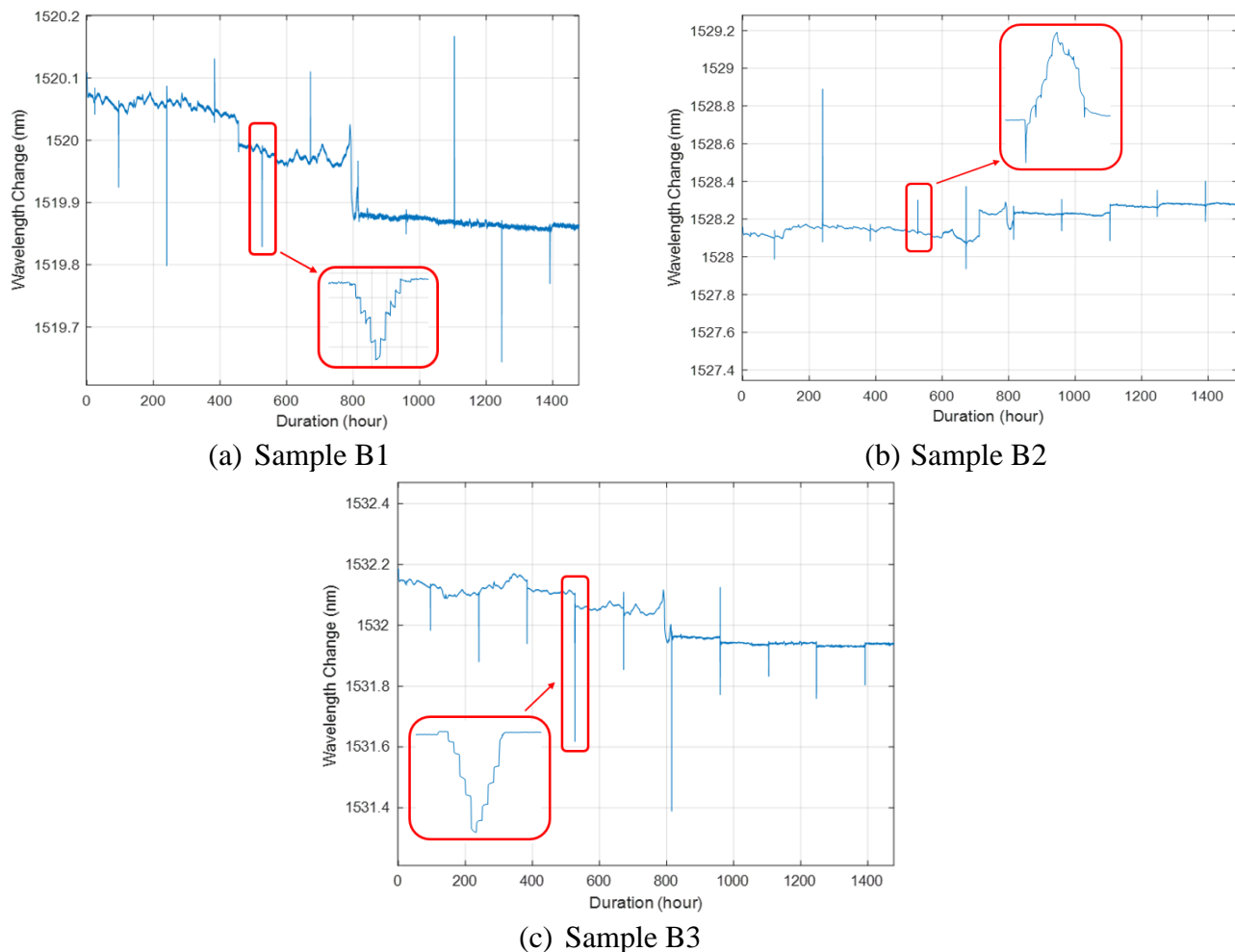
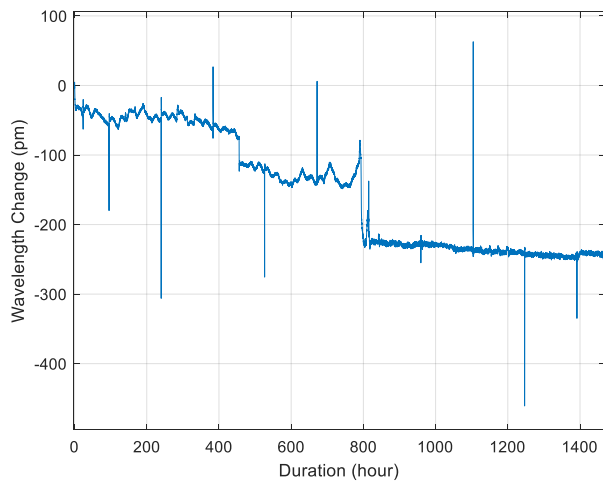
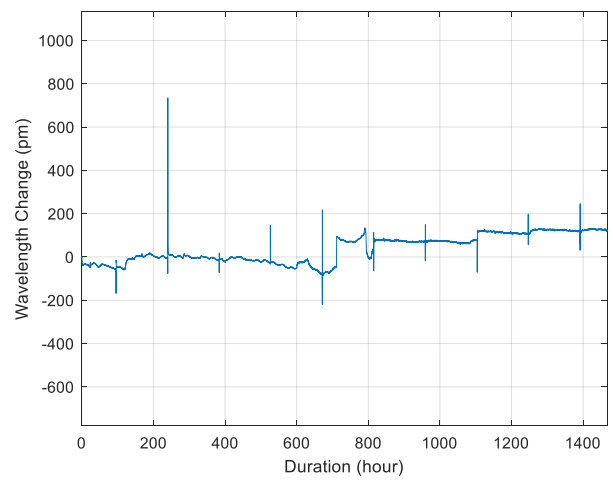


Fig. 15. Wavelength shifts of B1, B2 and B3 before temperature compensation.

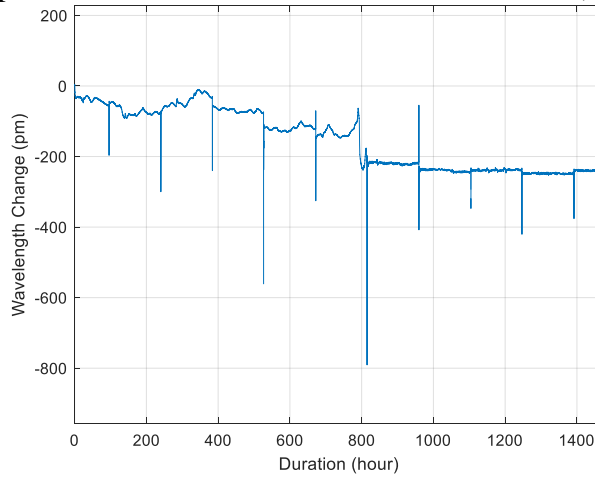
In Fig. 16, the initial measurement of the wavelength of each sensor was not zero. In order to manifest the shift of the wavelength of the FBG sensors during the testing, the measurement data were processed by compensating the initial reading. Therefore, each measured wavelength vs. time curve can be shifted to achieve a zero wavelength change at time zero. The processed results are shown in Fig. 16. Temperature compensation is not performed yet for the data in Fig. 16. The data from the sensor B2 seem abnormal because the data show a different trend from the trends shown by the other FBG sensors. The abnormal data might be related to external forces applied during the loading test. Further analysis is needed to understand the reasons.



(a) Sample B1



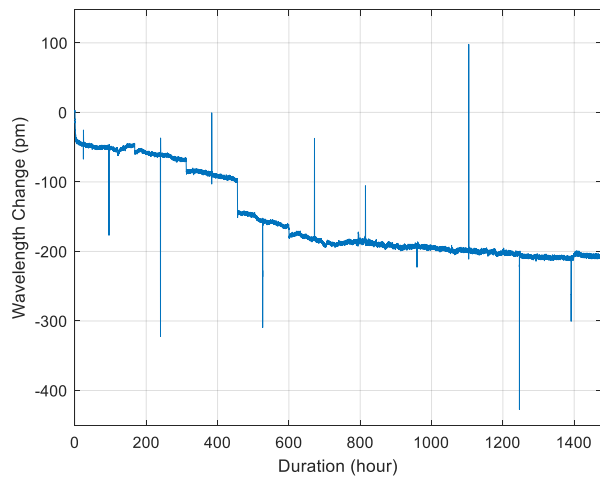
(b) Sample B2



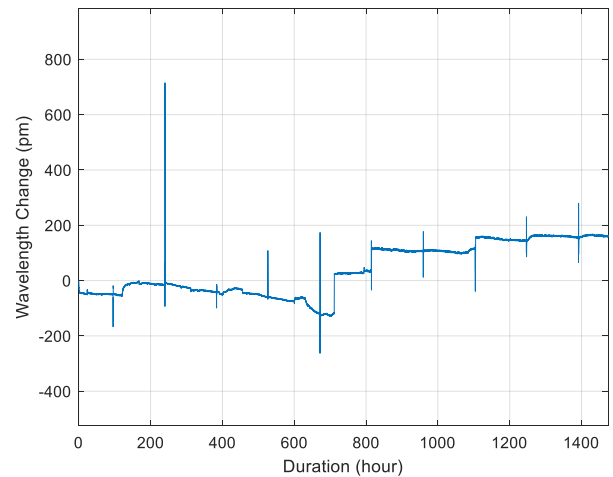
(c) Sample B3

Fig. 16. Wavelength shifts from zero of B1, B2 and B3 before temperature compensation.

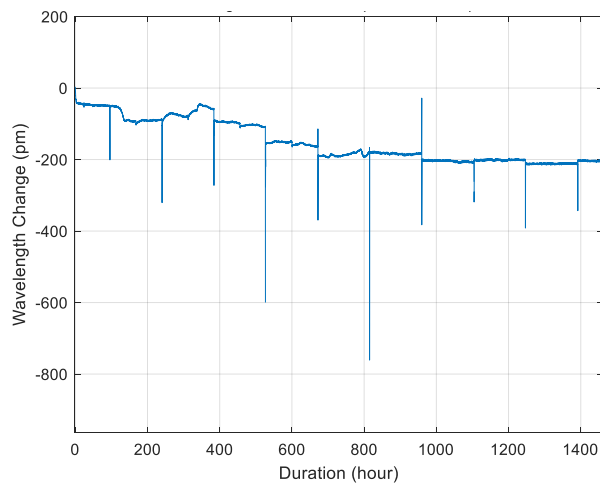
After temperature compensation, the wavelength shifts still exhibited the same changing laws as before temperature compensation, except that the unnecessary small peaks, that is, the temperature-induced wavelength shifts, were removed, as shown in Fig. 17.



(a) Sample B1



(b) Sample B2



(c) Sample B3

Fig. 17. Wavelength shifts from zero of B1, B2 and B3 after temperature compensation.

Comparing multiple wavelength shifts, it could be found that at the beginning, there was an overall downward trend because adding the 3.5wt% sodium chloride (NaCl) solution to simulate the corrosive environment was equivalent to applying a uniform load. Meanwhile, the slight fluctuations at the 24th hour were caused by making cracks. And at the 240th (10th day), SB2 had the opposite changing trend from the other two samples, as shown in Fig. 18. The reason is that during the third loading test, the stainless-steel loading frame reversed, and the severe external force applied on the steel plate. This led to premature separation of the coating (epoxy) from the steel plate so that the wavelength shifts gradually increased.

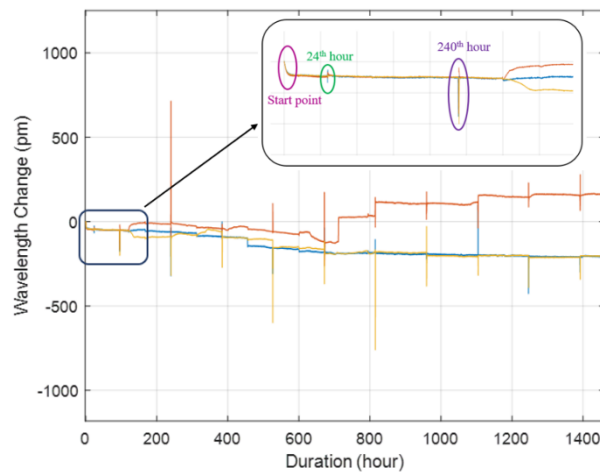


Fig. 18. Compare multiple wavelength shifts after temperature compensation.

(f) Task IV: Student Training and Reporting

In Task IV, we trained two graduate students (one from Stevens and one from NDSU) and two undergraduate students. Through the research, the students will be trained to become future experts in the related fields. In the fourth quarter, Task IV was performed to train two graduate students and two undergraduate researchers to conduct laboratory testing of the distributed fiber optic sensors. Two undergraduate students from Stevens were mentored by the PI to conduct research on the proposed topic, which was partially supported by the Pinnacle Scholar Program at Stevens Institute of Technology.

(g) Future work

In the sixth quarter, there will be three objectives:

- 1) Focus on the remaining activities planned in Task I: Developing and Characterizing Distributed Fiber Optic Sensors. Based on the laboratory testing of the distributed fiber optic sensors, we will conduct further experiments on using the optical fiber as distributed sensors to detect and quantify corrosion effects.
- 2) Focus on the remaining activities planned in Task II: Developing and Characterizing Point Fiber Optic Sensors. We will conduct laboratory testing of the point fiber optic sensors under various effects of anomalies of pipelines. Specifically, we will characterize the sensitivity of the point fiber optic sensors under multiple individual types of defects.
- 3) Focus on the remaining activities planned in Task IV. We will continue the efforts of training graduate and undergraduate students. In addition, a collaborative relationship has been recently initiated between Stevens Institute of Technology and multiple high schools in New Jersey. Multiple high school students will participate in some research activities related to this project.

References

[1] Luna ODiSI 6100 Multichannel Optical Distributed Sensor Interrogator. <https://lunainc.com/wp-content/uploads/2017/11/LUNA-ODiSI-6000-Data-Sheet.pdf>.